Preprint
UCRL-JC-152363

Studies of Indirect Drive IFE Capsules in Two and Three Dimensions

A.E. Koniges, M.M. Marinak, M. Tabak, M.C. Herrmann

This article was submitted to the
IFSA Conference, Monterey, California, September 7-12, 2003

September 2003

Studies of Indirect Drive IFE Capsules in Two and Three Dimensions

A. E. Koniges, M. M. Marinak, M. Tabak, and M. C. Herrmann
Lawrence Livermore National Laboratory, Livermore, CA 94551

Abstract
We study in detail the properties of a 265eV peak temperature indirect drive IFE capsule design. The capsule has a plastic ablator covering a layer of DT ice; with a DT gas fill and an outer radius of 2.3 mm. We give linear growth rate curves for single modes for a range of wave numbers, paying particular attention to the reduction of "chevron modes" that can occur as a result of numerical instabilities. We compare the two and three-dimensional behavior of single modes.

1. Introduction

Recent advances in computational capability have afforded the opportunity to study IFE capsule implosion characteristics in three dimensions. However, three-dimensional simulations, besides being much are computationally intensive than typical 2D simulations, are subject to a much wider variety of numerical instabilities due to the increased degrees of freedom in moving from a discretization of the capsule's physical space from planar cells to three-dimensional cells. In this paper we give details of a "test problem" for linear growth rates whereby we study the evolution of a very small perturbation on the outside ablator of the capsule and watch the time evolution of the linear growth phase at the fuel-ablator interface for various modes. For each mode studied, we vary the simulation characteristics to assure the sinusoidal mode shape imposed on the outer ablator surface remains in tact as it transfers to the fuel ablator interface and grows approximately three orders of magnitude before implosion. Then, we increase the initial magnitude of the perturbation (up to the magnitude assumed for typical surface roughnesses for manufactured capsules) to note the onset of the nonlinear saturation phase. Finally, we use these simulation parameters to design the grid and other aspects of the simulation for our 3D studies.

II. Hydrodynamics

Our typical capsule design, suitable for IFE-scale reactions has a plastic ablator covering a layer of DT ice, with a DT gas fill and an outer radius of 2.3 mm. The capsule is radiatively driven with a foot temperature of 80 eV and a peak temperature of approximately 265 eV. The capsule drive is given in Fig. 1.

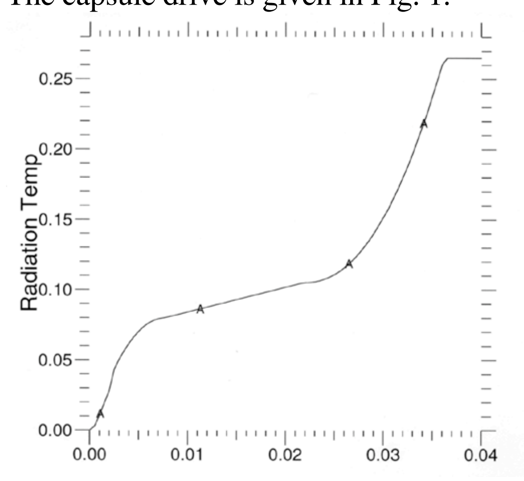

Figure 1. Radiation temperature in KeV imposed on the surface of the capsule as a function of time in microseconds.

The hydrodynamics of the capsule implosion is illustrated in Fig. 2, where we show color contours of log of the pressure as a function of time. The interfaces of ablator/fuel and fuel/gas are noted as fixed horizontal lines. We see that the first shock from the imposed radiation field enters the fuel at approximately 17ns and the fuel/gas interface at 31 ns.

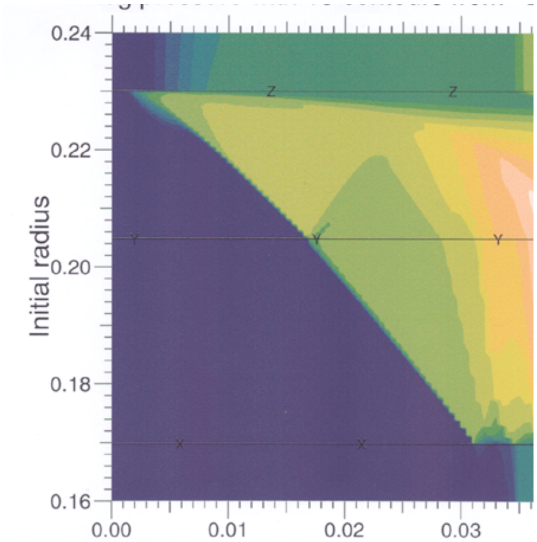

Figure 2. Log pressure contours as a function of initial radius and time in micro-sec show shocks entering the various layers and rarefactions rebounding. Line z labels the ablator, line y labels the ablator fuel interface, and line x labels the fuel/gas interface.

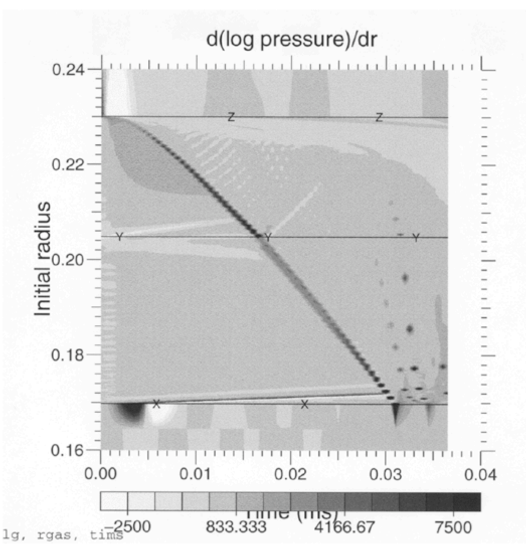

Figure 3. Derivatives of the log of the pressure show shock paths.

The derivative of the log of the pressure (Fig. 3) shows the actual shock trajectory. We note that these trajectories are sensitive to the opacity models used. This is important because in order to study three-dimensional configurations, we may want to use simplified opacity models to speed the calculation. Figure 4 shows the use of a slightly different opacity model (with the same radiation drive). Here, the shock timing is no longer optimized. We note that with each different opacity model used it may be necessary to "re-tune" the radiation drive on the capsule to assure that shocks do not combine in the fuel (thus degrading yields).

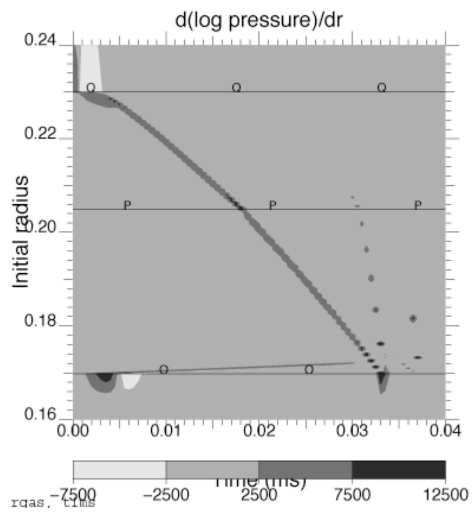

Figure 4. Use of slightly different opacity models can change the shock timing.

III. Linear Growth

To study the effect of hydrodynamic instabilities, we follow the evolution a very small perturbation imposed on the outside of the ablator. The perturbation is sinusoidal with a peak-to-peak variation of 2.0e-9 cm as is typically assumed to calculate linear growth factors. Figure 5 shows the time evolution of the perturbation normalized to its initial value for a scan of mode numbers ranging from l=40 to l=150. The peak-to-peak perturbation amplitude is measured at the fuel/ablator interface.

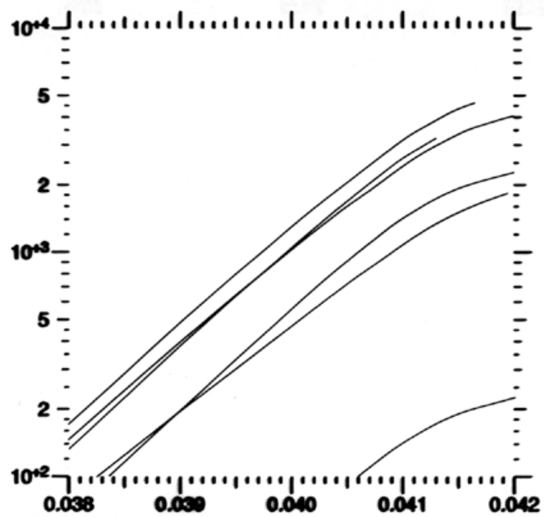

Figure 5. Linear growth rate curves for modes ranging from 40 to 150. The curves show the peak-to-peak variation vs. time measured at the fuel/ablator interface.

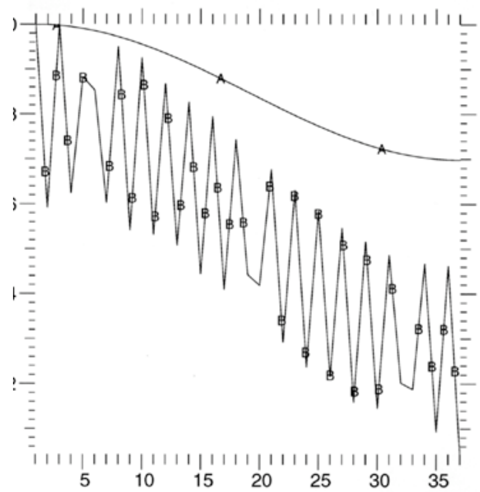

Figure 6. A sinusoidal perturbation can degrade rapidly if noise growth takes over the calculation. Curve A is a well-behaved perturbation and Curve B shows noise at .5ns later.

The fastest growing mode is l=80, with modes 60 and 100 having comparable growth rates and modes 40 and 120 also comparable, but significantly lower. Mode 150 grows very slowly.

For each mode, we are careful to track the sinusoidal structure of the perturbation until at least the time of peak implosion velocity, which occurs at approximately 40.6ns. Figure 6 shows how the growth of numerical instabilities leading to improper estimations of the growth rate can manifest itself. Here, for mode l=60 we show a well-behaved sinusoidal mode (curve A) that degrades rapidly into a degenerate numerical instability (curve B) in .5 ns. In this case, the instability is triggered by the use of tabular opacities instead of more smoothly generated opacity functions. We see similar behavior when the grid cells are not appropriately sized or when other simulation parameters are not appropriately adjusted so as to inhibit the introduction of noise.

IV. Nonlinear Regime

In typical capsule implosions, surface roughness is much larger than that given in our linear growth studies. In Fig. 7, we show the growth of the fastest growing mode (l=80) as we increase the initial perturbation peak-to-peak amplitude by steps of an order of magnitude, going from 2.0e-9 to 2.e-5 cm. The curves for 2.e-9 and 2.e-8 are indistinguishable, however, a noticeable reduction in the growth is evident for 2.e-5.

V. Three-dimensional Simulations

Finally, we start to explore the three dimensional space. Here, our typical simulations go from requiring only a day or so of computer time to weeks of computer time on approximately 64 processors of the ASCI-White computer system. In Figure 8, we give a comparison of the two-dimensional and three-dimensional density contours at 40 and 41 ns, just spanning the time of peak implosion velocity. We see that as expected, the three-dimensional symmetric perturbations grow faster than the corresponding 2D ones. We are currently examining filters and other techniques to assure that multi-mode simulations in 3D are similarly free of artificial growth imposed by numerical instabilities.

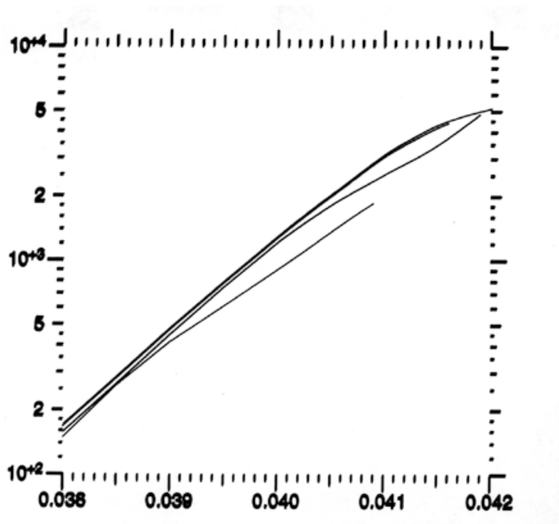

Figure 7. Mode growth for l=80 as the perturbation is increased in steps of an order of magnitude.

Lastly, in Figure 9, we show the three-dimensional mode shape of l=40 combined with l=160 repeated several times on a wedge of the capsule surface. Our future simulations will investigate mode-coupling and multi-mode simulations in 3D.

VI. Acknowledgments

This work was performed under the auspices of the U.S. Department of Energy by the University of California, Lawrence Livermore National Laboratory Under Contract No. W-7405-Eng-48.

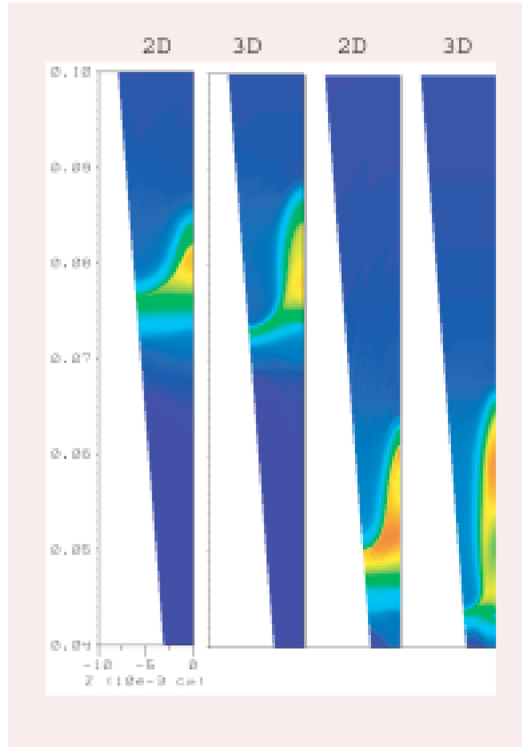

Figure 8. Comparison of 2D and 3D growth using density contours just before and after peak implosion velocity at t=40 and 41 ns.

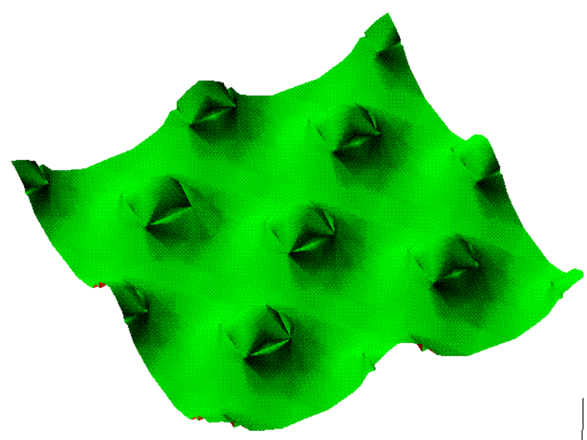

Figure 9. Three-dimensional growth shown on a surface wedge at the fuel/ ablator interface.